

Study of Bubble Activity in a Megasonic Field Using an Electrochemical Technique

Manish Keswani, Srinu Raghavan, and Pierre Deymier

Abstract—In the megasonic cleaning of wafers, size and motion of cavitating bubbles and fluid flow due to acoustic streaming play a very important role. In this paper, chronoamperometric technique has been used to seek information on acoustic streaming and bubble activity in a 1 MHz sound field. Specifically, current transients during reduction of potassium ferricyanide were recorded. Data collected at 1–6 MHz sampling rate using a 25 μm platinum electrode show current “peaks” indicative of the approach of oscillating bubbles to the electrode and current “valleys” due to blocking of the electrode by bubbles. Acoustic streaming velocity (~ 1.5 cm/s) and bubble size (maximum radius of ~ 1 μm for oscillating bubbles) have been estimated from local current transients caused by bubble activity near the electrode.

Index Terms—Acoustic streaming, bubble size, chronoamperometry, megasonic, wafer cleaning.

I. INTRODUCTION

THE USE OF megasonic energy for the removal of particles and other contaminants during wafer cleaning is widely practiced [1]. The parameters that are used to control the efficiency of particle removal in megasonic cleaning include sound frequency, transducer intensity, cleaning solution chemistry, process time, and temperature [2], [3]. The acoustic field parameters affect acoustic streaming and bubble cavitation, which play a critical role in particle removal [4], [5].

Acoustic streaming refers to steady fluid motion due to the loss of acoustic momentum caused by viscous attenuation and wave interactions with solid boundaries. There are mainly three types of acoustic streaming, namely Eckart streaming, Schlichting streaming, and microstreaming. Microstreaming is related to cavitation and occurs due to oscillating bubbles acting as secondary sources of sound. It often results in significant fluid movement and can be instrumental in particle removal during megasonic cleaning. Fig. 1 is a simple schematic representation of particles getting dislodged from the surface due to microstreaming effects from an oscillating bubble approaching the surface.

Manuscript received March 13, 2011; revised August 4, 2011; accepted August 10, 2011. Date of publication August 30, 2011; date of current version November 2, 2011. This work was supported by the National Science Foundation, under Award ID 0925340.

The authors are with the Department of Materials Science and Engineering, University of Arizona, Tucson, AZ 85721 USA (e-mail: manishk@email.arizona.edu; srini@u.arizona.edu; deymier@u.arizona.edu).

Color versions of one or more of the figures in this paper are available online at <http://ieeexplore.ieee.org>.

Digital Object Identifier 10.1109/TSM.2011.2165973

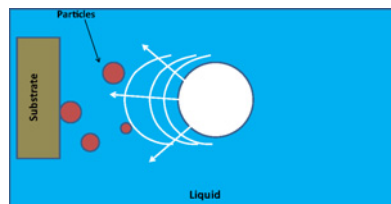


Fig. 1. Schematic showing dislodgment of particles from the surface due to microstreaming effects from an oscillating bubble approaching the surface.

There have been several studies [6]–[8] that have experimentally measured streaming velocities using different techniques. These studies show occurrence of streaming velocities typically in the range of 0–1.5 cm/s in water for megasonic frequencies of 0.5–4 MHz. For example, particle image velocimetry studies have shown a maximum acoustic streaming velocity of 1 cm/s in water at 0.95 MHz megasonic frequency [6]. In another study, laser Doppler velocimetry was employed to measure the fluid motion due to acoustic streaming and streaming velocities in the range of 0.3–1.1 cm/s were reported for megasonic frequencies of 2.98 and 3.46 MHz [7].

Acoustic cavitation, on the other hand, is related to the formation of stable and transient cavities when the fluid is subjected to an oscillating pressure field. Stable cavitation entails small oscillations of bubbles about an equilibrium size for many acoustic cycles and may lead to microstreaming. Determination of bubble size distribution is important for characterizing stable cavitation. Lee *et al.* used sonoluminescence technique and computed the bubble size distribution to be in the range of 2.8–3.7 μm in water for acoustic frequency of ~ 0.5 MHz [9]. Other techniques such as laser light diffraction [10] and active cavitation detection [11] have also been used to measure bubble sizes in water. The second type of cavitation, called transient cavitation, on the other hand, involves large bubble size variations, often for less than one cycle, and eventual bubble collapse, resulting in the formation of microjet or shock waves. Kornfeld and Suvorov were the first one to suggest that cavities collapse asymmetrically and proposed that liquid jets are formed when a collapse occurs close to a solid surface [12]. Other researchers have used numerical methods to predict the collapse of vaporous bubbles lacking spherical symmetry and obtained liquid jet velocities in the range of 130–170 m/s [13].

Although considerable work has been done to understand the phenomena of acoustic streaming and cavitation, reported

investigations on experimental characterization of single bubble activity in megasonic fields are very limited. One of the reasons for this is the requirement of a high speed experimental technique that can monitor the cavitation and streaming effects that typically occur in millisecond to microsecond time scale. Birkin *et al.* were amongst the first few to investigate mass transfer effects due to cavitation and streaming [14], [15] in an ultrasonic field (20–100 kHz) using chronoamperometry and cyclic voltammetry on a 6–25 μm microelectrode (C/Pt/Au). The current-time transients, due to single cavitation events, were observed to last for a few milliseconds. They concluded that micro-jetting resulting from bubble collapse contributed to the current spikes that lasted for a few milliseconds. More recently, a new insight into understanding of single bubble behavior was provided using a platinum microelectrode array (ranging from 25 μm to 0.5 mm in diameter) for both ultrasonic (20 kHz) and megasonic (0.5 MHz) frequencies [16], [17]. It was shown that hemispherical bubbles in the size range of 15–0.8 mm oscillating at harmonics and sub-harmonics of the driving frequency (20 kHz) had a life time of several milliseconds. At life times of the order of milliseconds, formation of microjet (which has a life time of a few microseconds [18]) was not possible and therefore its occurrence was ruled out. At acoustic frequency of 0.5 MHz, current transients were attributed to flux of solution toward the electrode surface due to microstreaming caused by bubble oscillations ($\sim 1 \mu\text{m}$ oscillation amplitude for resonating bubble of 6 μm in size) with life time of tens of milliseconds.

It is apparent from aforementioned studies that high resolution electrochemical technique employing a microelectrode is very useful for characterizing cavitation and acoustic streaming [14]–[17]. This technique can provide important information on bubble behavior including its movement, oscillation, size, as well streaming effects generated by it. However, so far most of the work conducted using this technique has been in ultrasonic frequency range. Considering the fact that semiconductor industry uses megasonic frequencies for cleaning applications, this paper is aimed at the understanding of cavitation and acoustic streaming in a 1 MHz sound field. Using a 25 μm Pt microelectrode, chronoamperometric measurements have been conducted to understand bubble activity in real time and to estimate the local acoustic streaming velocity close to the electrode surface.

II. EXPERIMENTAL METHODS AND MATERIALS

Chemical reagents, potassium ferric cyanide (99.9% $\text{K}_3\text{Fe}(\text{CN})_6$) and potassium chloride (99.9% KCl) were purchased from Alfa Aesar and were used as received. Aqueous solutions containing 2 mM of $\text{K}_3\text{Fe}(\text{CN})_6$ and 0.1 M KCl (as supporting electrolyte) were prepared using ultrapure water of resistivity 18 $\text{M}\Omega\cdot\text{cm}$. Oxygen was removed from solutions as measured using an oxygen sensor (Rosemount Analytical model 499A DO) by bubbling argon gas for 30 min. After this period, argon gas blanket was maintained over the surface of the solution to prevent diffusion of oxygen back into the solution during the experiments, which were conducted at $23 \pm 2^\circ\text{C}$.

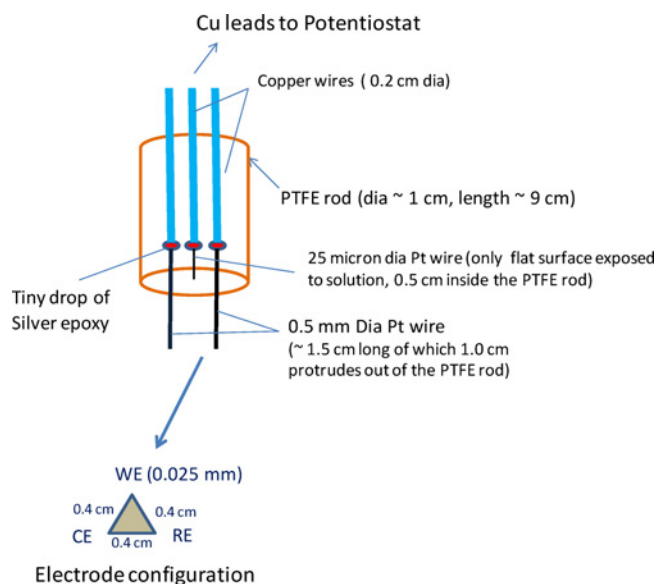


Fig. 2. Schematic of three electrode setup used for electrochemical experiments.

Electrochemical experiments were performed in a ferricyanide solution, with and without megasonic exposure, using a three-electrode arrangement. A schematic of the electrode setup is shown in Fig. 2. The working electrode used was a 25 μm diameter Pt disk electrode. Platinum wires of diameter 0.05 cm and length 1.0 cm served as counter and pseudo-reference electrodes. All three electrodes were mounted in a Teflon block in a triangular pattern with ~ 0.4 cm spacing between them. The back side of each electrode was connected to a 0.2 cm diameter copper wire (used as current lead) with a minute amount of silver epoxy to reduce any stray capacitance. Platinum and copper wires were of 99.99% purity and purchased from Goodfellow. Prior to each experiment, all electrodes were cleaned using room temperature nitric acid (reagent grade 70%) for 5 min followed by sulfuric acid (reagent grade 96%) for another 5 min. Electrodes were thoroughly rinsed with DI water and dried with N_2 blow after each cleaning step.

All experiments were conducted in a megasonic system provided by ProSys. The system consisted of a cylindrical polypropylene bowl, 8.9 cm in diameter and 9.5 cm in depth, containing a 1 MHz circular transducer of area 22.2 cm^2 that was covered with sapphire for chemical tolerance. All experiments were run at a power density of 2.0 W/cm^2 . The working electrode was positioned close to the center of the transducer but moved at different locations in the vertical direction to obtain current transients with different degree of cavitation activity. A liquid fill height of 3 cm was maintained approximately constant in all the experiments.

Chronoamperometry experiments were conducted using a Princeton Applied Research potentiostat PARSTAT 2273 which has a minimum rise time of 0.25 μs , current resolution of 1.2 fA, and current sampling rate of ~ 15 Hz. This potentiostat allows filtering of the current if necessary to decrease the noise level. In most experiments, a single potential-step of either -0.8 or -1.2 V was applied to the working electrode (with respect to platinum reference) and current was measured

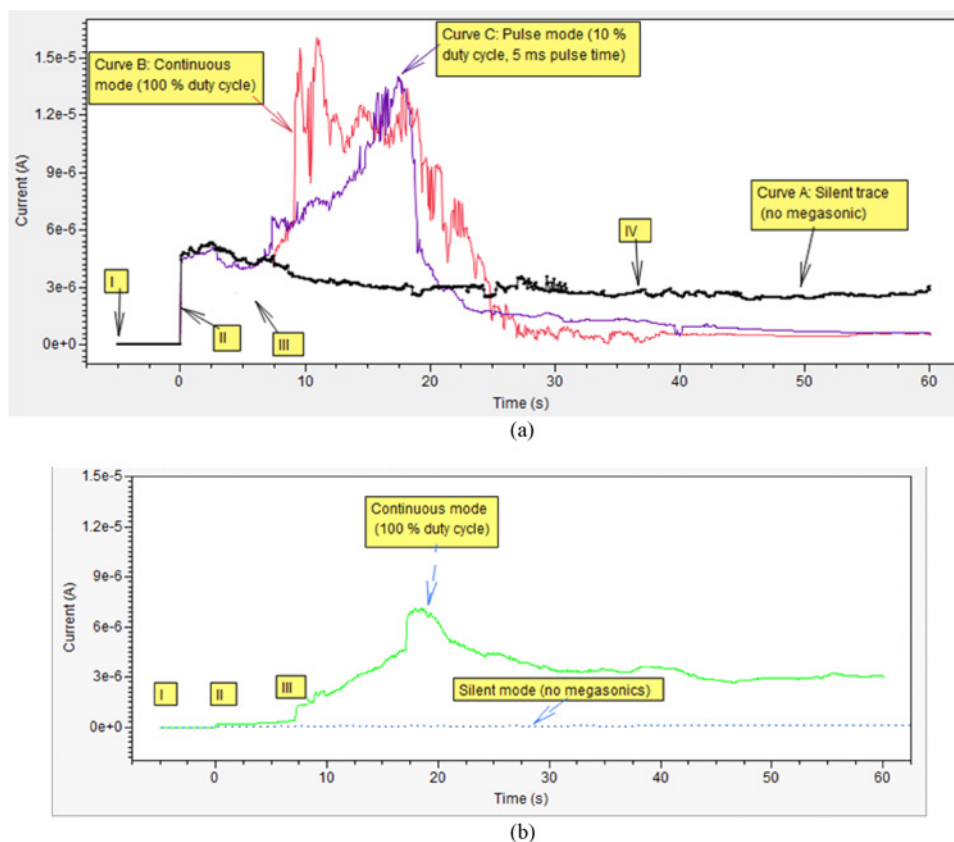


Fig. 3. (a) Plot showing current (~ 15 Hz sampling rate) as a function of time recorded at $25 \mu\text{m}$ microelectrode for applied potential-step of -1.2 V (versus Pt reference) in aqueous solution of $2 \text{ mM K}_3\text{Fe}(\text{CN})_6$ and 0.1 M KCl . The markers I to IV are explained in the text. (b) Plot of current versus time for similar conditions as (a) except that the applied potential-step was -0.8 V (versus Pt reference).

as a function of time. In some of the initial experiments, measurements were first made for 5 s without application of potential and this was followed by a potential-step of -0.8 or -1.2 V and the current was recorded for ~ 6 s. After that the transducer was turned on for 30 s, in either continuous (100% duty cycle, 50 ms pulse period) or pulse mode (10% duty cycle, 5 ms pulse period). The entire measurement lasted for about 65 s. The temporal variation of current was also recorded using an external oscilloscope NI USB-5133 at a sampling rate between 1 and 6 MHz. The data acquisition at such high sampling rates, however, limited the total capture time to less than 1 s. Labview 9.0 was used to acquire and write the data from the oscilloscope, which was processed for graphical output using SAS JMP 8 software.

III. RESULTS AND DISCUSSION

Chronoamperometric experiments were performed in aqueous solutions of potassium ferricyanide at a potential of -1.2 V in the absence and presence of 1 MHz sonic field. Fig. 3(a) shows the current recorded under low resolution conditions (15 Hz sampling rate) for a total measurement time of 65 s as curves A, B, and C. Curve A corresponds to no megasonic condition, and B and C to continuous and pulse modes of sound excitation, respectively. Initially between time $t = -5$ s (point I) and $t = 0$ s (point II), no potential was applied and hence the current value was zero. At point II, a

potential-step of -1.2 V was imposed and the current jumps to a steady-state diffusion limited baseline value of about $4 \mu\text{A}$. In the absence of megasonics (curve A), the current drops slightly and eventually stays approximately constant for the entire period during which the potential is applied. When the transducers were turned on at a time marked by III (in the case of curves B and C), the current increases to about three times the initial steady-state value and then decreases and finally reaches another quasi steady-state value lower than the steady state current for curve A (no megasonics). The increase in baseline current on application of megasonic energy may be attributed to the bulk flow of solution toward the electrode surface brought by the acoustic streaming. The decrease in acoustic streaming current after a certain time is believed to occur when a bubble adhering to the electrode (which probably restricts its oscillatory movement) gradually gets bigger and blocks electrode surface to a significant extent and leads to a situation where the current falls below the diffusion limited current. This suggests that the shape of the bubble is a deformed sphere, as also reported in some of the recent literature [19], [20]. It is also important to point out that there does not appear to be much difference in the overall acoustic streaming current between the continuous and pulse modes of sound excitation, as apparent from profile of curves B and C. When current was sampled in the MHz range, current transients were found to be superimposed on the acoustic streaming current. This will be discussed later.

In some cases, as shown in Fig. 3(b) the measured current during the transducer on time was higher than the current measured in the absence of megasonic field. In Fig. 3(b), the dotted line corresponds to the chronoamperogram for a potential step of -0.8 V in the absence of megasonic field while the solid one represents that obtained in the presence of megasonic irradiation. The higher value of current during the entire period (7–60 s) of megasonic exposure indicates that the electrode surface is free of any adhering bubbles unlike in the case shown in Fig. 3(a).

The effect of using a high sampling rate of 1 MHz on current-time data is shown in Fig. 4(a). The data in this figure was collected at applied potential-step of -1.2 V after the transducer was turned on and during the time period marked by III and IV (notations explained in earlier section). Superimposed on the acoustic streaming current are current “valleys” these are most likely due to blocking of the electrode surface as a bubble moves in close vicinity of the electrode thereby restricting the flux of solution toward the electrode surface. The rate at which current falls probably reflects the bubble movement caused by convective fluid flow close to the electrode surface. For the three current “valleys (V1, V2, and V3)” shown in Fig. 4(a) (insets show expanded view of “valleys”), although the current fall time is different (0.4–1.7 ms) for each, the rate at which the current falls is about the same ($\sim 5.0\text{--}6.0 \times 10^{-3}\text{ A/s}$). After the current falls to the lowest value, it starts to recover back to the acoustic streaming current. The recovery time for current may include time taken by the bubble to move away from the electrode as well as the time for relaxation of the diffusion layer after the bubble leaves. Since the area of the electrode covered by the bubble will depend on the size of the bubble, the depth of the valley may also be expected to depend on the bubble size. In the case of “valley V1,” where the current drops below the baseline current value under no megasonic condition ($\sim 4\text{ }\mu\text{A}$), the bubble covering the electrode surface must be about the same size as the electrode or larger. However, if the bubble size was much larger than the electrode, one would expect that the bubble would entirely cover the electrode for some time as it moves across it and therefore the current would stay constant at a low value during that time. Since the recovery of current begins immediately after fall, it is quite likely that the bubble in the case of “valley V1” is approximately of the same size ($25\text{ }\mu\text{m}$) as the electrode. Making the assumption that the distance traveled by the bubble as it moves across the electrode is approximately equal to the diameter of the electrode, the bubble speed representing local (near the electrode surface) fluid velocity can be estimated by dividing the diameter of the electrode by the current fall time (1.7 ms) for “valley V1.” This gives the local fluid velocity to be $\sim 1.5\text{ cm/s}$. The calculated value agrees reasonably well with that obtained by other researchers using non-electrochemical techniques [6], [7]. Fig. 4(b) shows another example of “current valleys” obtained under similar experimental conditions as that for data in Fig. 4(a). The rate at which the current falls in these valleys is between $3.0 \times 10^{-3}\text{ A/s}$ and $6.0 \times 10^{-3}\text{ A/s}$, suggesting that streaming velocities are in the same range as that calculated in the previous section. The mean of all the current fall rates

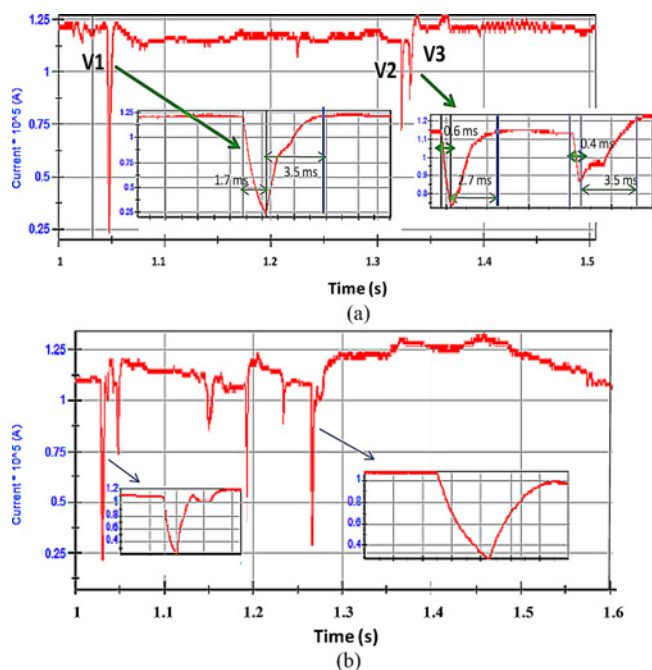


Fig. 4. (a) Chronoamperometric results obtained on 2 mM $\text{K}_3\text{Fe}(\text{CN})_6$ and 0.1 M KCl solution, irradiated with $\sim 1\text{ MHz}$ frequency, while holding the microelectrode ($25\text{ }\mu\text{m}$) at -1.2 V versus Pt and recording the current at a sampling rate of 1 MHz. (b) Chronoamperometric results obtained for experimental conditions similar to that used to obtain data in Fig 4(a).

observed for different sets of experiments performed in this paper was $\sim 5 \pm 1.5\text{ A/s}$.

A bubble oscillating with significant amplitude near the electrode could lead to enhanced fluid flow (mass transfer) toward the electrode, thereby yielding current “peaks” superimposed on baseline current due to acoustic streaming. Fig. 5 shows such current peaks recorded for a potential step of -1.2 V in the presence of 1 MHz sound field. The current first rises to a maximum (peak) value, stays constant at this value for a few milliseconds, and then decays back to the reference value of acoustic streaming current. These peak currents lasted between 15 and 50 ms with rise time varying from 3 to 10 ms. Considering the millisecond time scale of the current rise, it may represent approach of an oscillating bubble from the bulk of the solution to the electrode surface [17]. At the same time, the magnitude of current values would represent enhanced mass transfer due to fluid displacement to the electrode surface due to the oscillations of the bubble. Similarly, the current decay time may represent bubble moving away from the electrode. Fig. 6 illustrates transport of ferricyanide species toward the electrode surface due to convective fluid flow generated by microstreaming from an oscillating bubble approaching the electrode. Initially when the bubble is far from the electrode, microstreaming effects are not felt by the electrode surface. As the bubble gets closer to the electrode, fluid displacement due to oscillations of the bubble causes upsurge of ferricyanide concentration at the electrode surface resulting in observed current “peaks.” Another possibility is that increase in current is due to increasing amplitude of oscillation of a bubble near the electrode as the bubble grows (due to rectified diffusion [21]) from a smaller size to close to its resonant size.

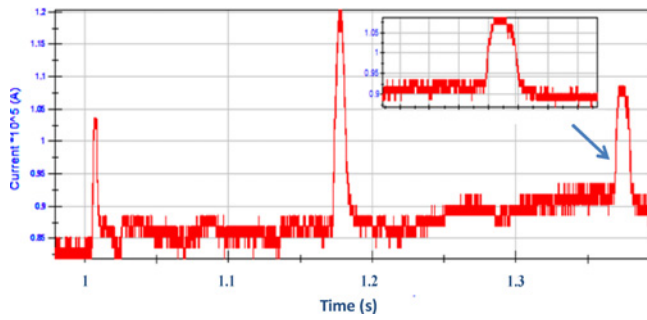


Fig. 5. Single cavitation bubble transient chronoamperometric current (sampling rate ~ 6 MHz) recorded using a $25 \mu\text{m}$ Pt microelectrode for a 2 mM potassium ferricyanide solution. Electrode potential: -1.2 V (versus Pt ref.), megasonic frequency ~ 1 MHz.

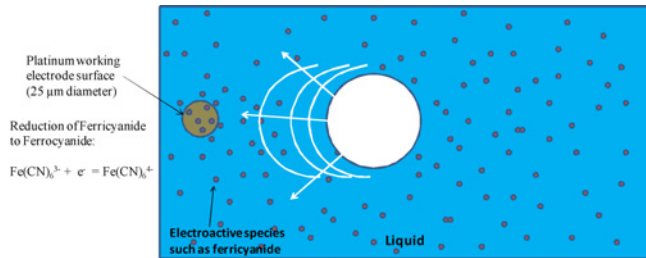


Fig. 6. Illustration of transport of ferricyanide species toward the electrode surface due to convective fluid flow generated by microstreaming from an oscillating bubble approaching the electrode.

Maisonhaute *et al.* [17] estimated the size of the bubble using a simple procedure and the same method is adopted here. The current due to microstreaming, as obtained from the peak height in Fig. 5, ranged between 1.0 and $3 \mu\text{A}$ (which also corresponded to maximum value of peak height current measured for all the experiments conducted with this electrode). Converting this current range into corresponding charge in one acoustic cycle gives a charge value of 1×10^{-12} – 3×10^{-12} C. Since the concentration of electroactive species used in experiments was 2 mM, a charge of 1×10^{-12} – 3×10^{-12} C would be contained in a liquid volume of 5 – $16 \mu\text{m}^3$. Assuming, the bubble contracts close to zero radius during its oscillation, a fresh solution of volume 5 – $16 \mu\text{m}^3$ equal to the volume of one bubble would be introduced at the electrode surface. This would yield bubble radii in the range of 1.1 – $1.6 \mu\text{m}$. These bubble radii values are quite reasonable considering that the resonant size of bubble is $\sim 3.5 \mu\text{m}$ at 1 MHz sound frequency.

In the above method to estimate bubble radii, it was assumed that the oscillating bubble shrinks to zero radius during contraction. This assumption may not be true. Using the linear theory of small oscillations of gas bubble [22], [23], one can estimate the bubble sizes and the corresponding oscillation amplitudes that will yield a liquid displaced volume of 5 – $16 \mu\text{m}^3$. The oscillation amplitude (ξ_{b0}) and a dimensionless parameter, δ , indicative of contribution to damping of bubble oscillation from viscous dissipation are given by the following equations:

$$\xi_{b0} = [P_a^* R_0 / (3^* \gamma^* P_0)] [(1 - (\omega/\omega_r)^2)^2 + (\omega/\omega_r)\delta^2]^{-0.5}$$

and

$$\delta = 4^* \eta / (\rho \omega_r R_0^2)$$

respectively.

In these equations, P_a is the gauge pressure (2.15 atm) for the power density of 2 W/cm^2 , P_0 is the atmospheric pressure, R_0 is the mean radius of the oscillating bubble, $\gamma (= 1.67)$ is the ratio of the specific heat at constant pressure to that at constant volume for the gas (argon) dissolved in the experimental solution, η and ρ are the viscosity and density of the solution, ω is the angular driving frequency and ω_r is the angular resonant frequency corresponding to radius R_0 . The terms ω_r and R_0 are related by the equation $\rho \omega_r^2 R_0^2 = 3\gamma(P_0 + 2\sigma/R_0) - 2\sigma/R_0$, where σ is the surface tension of the solution. First, ξ_{b0} and δ were calculated for different values of bubble radii, R_0 . The computed values of ξ_{b0} were then used to calculate the maximum and minimum radii of oscillating bubbles as $R_0 + \xi_{b0}$ and $R_0 - \xi_{b0}$, respectively. The volume of liquid displaced due to oscillating bubble was calculated from the maximum and minimum radius of bubble. These calculated values for different bubble radii were compared with previously computed liquid displaced volume of 5 and $16 \mu\text{m}^3$. It was found that bubbles of radii of 0.7 and $1.1 \mu\text{m}$ with oscillation amplitudes of 0.35 and $0.54 \mu\text{m}$ (for δ values of 0.25 and 0.16, respectively) would yield liquid displacement volumes of ~ 5 and $16 \mu\text{m}^3$, respectively. Bubble sizes in this range have been reported in the literature for acoustic frequency of 1.1 MHz and were determined using active cavitation detection technique [11]. These results show that the electrochemical sensor (microelectrode) used in this paper is capable of probing oscillating bubbles with a maximum size of $\sim 1 \mu\text{m}$ in liquid exposed to a 1 MHz sound field.

This preliminary work has shown that bubble activity in a megasonic field can be probed using chronoamperometric technique. One of the benefits of this technique is that it can provide cavitation and streaming related details close to a surface (pertinent for megasonic wafer cleaning) as opposed to other techniques based on sonoluminescence and hydrophone which are mainly bulk measurements. However, to obtain information useful for wafer cleaning applications, investigations need to be conducted in different chemical cleaning solutions. Additionally, the technique in its present form is limited to measurements at one location at a time in the solution. This shortcoming can be eliminated by employing a microelectrode array, which can provide information at several locations with respect to the megasonic transducer.

IV. CONCLUSION

High resolution electrochemical technique employing microelectrode has been used to monitor cavitation and acoustic streaming during exposure of a liquid to a high frequency sound field. The choice of megasonic frequency of 1 MHz for investigations in this paper was based on its relevance to wafer cleaning applications for integrated circuit industry. Current transients due to microstreaming caused by bubble oscillation were found to be superimposed on acoustic streaming current. Acoustic streaming velocity was computed to be $\sim 1.5 \text{ cm/s}$

from current “valleys” observed due to blocking of the electrode by the bubbles. The microelectrode used in this paper is capable of probing oscillating bubbles with a maximum size of $\sim 1 \mu\text{m}$ in liquid exposed to sound field of 1 MHz frequency.

ACKNOWLEDGMENT

The authors would like to thank Prof. E. Maisonhaute, UPMC, Paris, France, for useful discussions.

REFERENCES

- [1] M. Keswani, S. Raghavan, P. Deymier, and S. Verhaverbeke, “Megasonic cleaning of wafers in electrolyte solutions: Possible role of electroacoustic and cavitation effects,” *Microelectron. Eng.*, vol. 86, no. 2, pp. 132–139, Feb. 2009.
- [2] K. Muralidharan, M. Keswani, H. Shende, P. Deymier, S. Raghavan, F. Eschbach, and A. Sengupta, “Experimental and simulation investigations of acoustic cavitation in megasonic cleaning,” *Proc. SPIE*, vol. 6517, pp. 65171E-1–65171E-13, Feb. 2007.
- [3] M. Keswani, “Megasonic cleaning of wafers in electrolyte solutions: Possible role of electroacoustic and cavitation effects,” Ph.D. dissertation, Dept. Chem. Environ. Eng., Univ. Arizona, Tucson, AZ, 2008.
- [4] V. Kapila, P. Deymier, H. Shende, V. Pandit, S. Raghavan, and F. Eschbach, “Megasonic cleaning, cavitation and substrate damage: An atomistic approach,” *Proc. SPIE*, vol. 6283, pp. 628324-1–628324-12, Apr. 2006.
- [5] G. Gale and A. Busnaina, “Roles of cavitation and acoustic streaming in megasonic cleaning,” *Particulate Sci. Technol.*, vol. 17, no. 3, pp. 229–238, 1999.
- [6] W. Kim, T. Kim, J. Choi, and H. Kim, “Mechanism of particle removal by megasonic waves,” *Appl. Phys. Lett.*, vol. 94, no. 081908, pp. 1–3, 2009.
- [7] S. Sakamoto and Y. Watanabe, “Effects of existence of microbubbles for increase of acoustic streaming,” *Japan. J. Appl. Phys.*, vol. 38, no. 5B, pp. 3050–3052, 1999.
- [8] T. Kuehn, D. Kittelson, Y. Wu, and R. Gouk, “Particle removal from semiconductor wafers by megasonic cleaning,” *J. Aerosol Sci.*, vol. 1, no. 1, pp. 427–428, 1996.
- [9] J. Lee, M. Ashokkumar, S. Kentish, and F. Grieser, “Distribution of the size distribution of sonoluminescence bubbles in a pulsed acoustic field,” *J. Am. Chem. Soc.*, vol. 127, no. 48, pp. 16810–16811, Dec. 2005.
- [10] F. Burdin, N. Tsochatzidis, P. Guiraud, A. Wilhelm, and H. Delmas, “Characterization of the acoustic cavitation cloud by two laser techniques,” *Ultrason. Sonochem.*, vol. 6, nos. 1–2, pp. 43–51, Mar. 1999.
- [11] W. Chen, T. Matula, and L. Crum, “The disappearance of ultrasound contrast bubbles: Observations of bubble dissolution and cavitation nucleation,” *Ultrasound Med. Biol.*, vol. 28, no. 6, pp. 793–803, Jun. 2002.
- [12] M. Kornfeld and L. Suvorov, “On the destructive action of cavitation,” *Japan. J. Appl. Phys.*, vol. 15, no. 6, pp. 495–506, 1944.
- [13] M. Plesset and R. Chapman, “Collapse of an initially spherical vapor cavity in neighborhood of a solid boundary,” *J. Fluid Mech.*, vol. 47, no. 2, pp. 283–290, 1971.
- [14] P. Birkin, C. Delaplace, and C. Bowen, “Electrochemical and photographic detection of cavitation phenomena within a variable frequency acoustic field,” *J. Phys. Chem. B*, vol. 102, no. 52, pp. 10885–10893, 1998.
- [15] P. Birkin and S. Silva-Martinez, “A study of the effect of ultrasound on mass transport to a microelectrode,” *J. Electroanal. Chem.*, vol. 416, nos. 1–2, pp. 127–138, 1996.
- [16] E. Maisonhaute, P. White, and R. Compton, “Surface acoustic cavitation understood via nanosecond electrochemistry,” *J. Phys. Chem. B*, vol. 105, no. 48, pp. 12087–12091, 2001.
- [17] E. Maisonhaute, F. J. Del Campo, and R. Compton, “Microelectrode study of single cavitation bubbles induced by 500 kHz ultrasound,” *Ultrason. Sonochem.*, vol. 9, no. 5, pp. 275–283, Oct. 2002.
- [18] K. Gandhi and R. Kumar, “Sonochemical reaction engineering,” *Sadhana*, vol. 19, no. 6, pp. 1055–1076, 1994.
- [19] J. Blake, G. Keen, R. Tong, and M. Wilson, “Acoustic cavitation: The fluid dynamics of non-spherical bubbles,” *Phil. Trans. R. Soc. Lond. A*, vol. 357, pp. 251–267, Feb. 1999.
- [20] N. Bremond, M. Arora, S. Dammer, and D. Lohse, “Interaction of cavitation bubbles on a wall,” *Phys. Fluids*, vol. 18, no. 121505, pp. 1–10, 2006.
- [21] D. Hsieh and M. Plesset, “Theory of rectified diffusion of mass into gas bubbles,” *J. Acoust. Soc. Am.*, vol. 33, no. 2, pp. 206–215, 1961.
- [22] F. Young, *Cavitation*. New York: McGraw-Hill, 1989, pp. 48–49.
- [23] W. Coakley and L. Nyborg, “Dynamics of gas bubbles,” in *Applications in Ultrasound: Its Applications in Medicine and Biology*, F. J. Fry, Ed. Amsterdam, The Netherlands: Elsevier, 1978, p. 109.



Manish Keswani received the Ph.D. degree in chemical engineering from the University of Arizona, Tucson, in May 2008.

He is currently an Assistant Research Professor with the Department of Materials Science and Engineering, University of Arizona. His current research interests include understanding the role of cavitation and acoustic streaming in megasonic processes for improvement of wafer cleaning (and reduction of damage) in microelectronics applications. He uses electrochemical, sonoluminescence, and acoustic emission (hydrophone) based techniques for his research activities.



Srini Raghavan received the Ph.D. degree in materials science and engineering from the University of California, Berkeley, in 1976.

He is currently a Professor with the Department of Materials Science and Engineering and with the Department of Chemical and Environmental Engineering, University of Arizona, Tucson. He applies electrochemical and surface chemical concepts for the understanding and improvement of wet chemical cleaning, etching (controlled corrosion), polishing, and passivation of surfaces. He has published close to 140 scientific papers and has five patents to his credit. His current research interests include corrosion of copper during integrated circuit manufacturing, study of cavitation phenomena during megasonic cleaning of semiconductor surfaces, and use of ionic liquids for surface cleaning.



Pierre Deymier received the Ph.D. degree in ceramics from the Massachusetts Institute of Technology, Cambridge, in July 1985.

He is currently the Head of the Department of Materials Science and Engineering and the Director of the School of Sustainable Engineered Systems, University of Arizona, Tucson. He was the Associate Head of the Department of Materials Science and Engineering from 2001 to 2010, and is on the faculty of the BIO5 Institute, Applied Mathematics Graduate Interdisciplinary Program, and the Biomedical Engineering Program. He has published more than 150 scientific papers and has presented at numerous technical meetings. His current research interests include the application of theory, modeling, and simulation to solving important problems in the science, engineering, and technology of materials. These areas of research include materials whose function derives from their size, such as nanomaterials, or structure, such as metamaterials, and materials with biological functionality or made of living matter, such as vitamaterials.